Single Molecule Magnets (SMM) Spin Channels Connecting FeMn Antiferromagnet and NiFe Ferromagnetic Electrodes of a Tunnel Junction

Babu Ram Sankhi[1], Erwan Peigney[1], Hayden Brown[1], Pius Suh[1], Carlos Rojas-Dotti[2,3], José Martínez-Lillo[2], Pawan Tyagi[*1]

Center for Nanotechnology Research and Education, Mechanical Engineering, University of District of Columbia, Washington, DC 20008, USA[1]

Departament de Química Inorgànica / Instituto de Ciencia Molecular (ICMol), University of Valencia, c/ Catedrático José Beltrán 2, Paterna (Valencia) 46980, Spain[2]

Área Química Inorgánica / Departamento Estrella Campos, Facultad de Química, Universidad de República, General Flores 2124, Montevideo, Uruguay[3]

Corresponding Author Email: ptyagi@udc.edu

Abstract:

The integration of single-molecule magnets (SMMs) into magnetic tunnel junctions (MTJs) offers significant potential for advancing molecular spintronics, particularly for next-generation memory devices, quantum computing, and energy storage technologies such as solar cells. In this study, we present the first demonstration of SMM-induced spin-dependent properties in an antiferromagnet-based MTJ molecular spintronic device (MTJMSD). We engineered cross-junction-shaped devices comprising FeMn/AlO_x/NiFe MTJs. The AlO_x barrier thickness where the exposed junction edges meet was comparable to the SMM length, facilitating the incorporation of SMM molecules as spin channels for spin-dependent transport. The SMM channels enabled long-range magnetic moment ordering around molecular junctions, which were precisely engineered via fabrication processes. The SMM, composed of a $[Mn_6(\mu_3\text{-}O)_2(H_2N\text{-}sao)_6(6\text{-}atha)_2(EtOH)_6]$ (H_2N-saoH = salicylamidoxime, 6-atha = 6-acetylthiohexanoate) complex, featured thioester groups at the ends that upon hydrolysis they form bonds with the magnetic electrodes. SMM-treated junctions demonstrated a significant current enhancement, reaching up to 7 μA at an input voltage of 60 mV. Furthermore, SMM-doped junctions exhibited current stabilization in the μA range at lower temperatures, whereas the bare electrodes showed current suppression to the picoampere range. Magnetization measurements conducted at 55 K and 300 K on pillar-shaped devices revealed a reduction in magnetic moment at low temperatures. Additionally, Kelvin probe atomic force microscopy (KPAFM) measurements confirmed that SMM integration transformed the electronic properties over long ranges. These findings are attributed to the spin channels formed between magnetic metal electrodes, which enhance spin polarization at each magnetic electrode. Our research highlights the potential of using antiferromagnetic materials, characterized by minimal stray fields and zero net magnetization, to transform MTJMSD devices.

Introduction:

Molecular spintronics devices (MSD), which leverage electronic spin in addition to charge, hold significant promise for advanced data storage and memory technology applications,

ranging from traditional computers to quantum computing, and offer numerous possibilities for exploring fascinating physical phenomena [1-6]. Molecules, due to their small size, mass reproducibility, and interesting quantum properties, are essential components in this field [7, 8]. In particular, single-molecule magnets (SMMs) consist of a central magnetic core surrounded by organic ligands (Fig. 1c), which can be customized to bind to surfaces or junctions [5, 9, 10]. The delocalized bonds within SMMs enhance magnetic interactions between central ions, improving their conductive properties. These molecules exhibit a diverse array of quantum phenomena, such as quantum tunneling of magnetization, Berry-phase interference, and quantum coherence, all of which are vital for advancing the understanding and development of spintronic devices [5, 11-13].

However, their functionalities can be fully explored only when they are effectively connected to metal electrodes. Various approaches have been used to construct MSDs, as documented in the literature [14, 15] [16]. Despite the success of these conventional approaches in demonstrating the feasibility of MSD devices, they come with several drawbacks, such as unsuitability for mass production [17], difficulties in using different magnetic electrodes [18] and damage to molecular channels during fabrication, resulting in atomic-level defects. Understanding the temperature-dependent properties of Single-Molecule Magnets (SMM) and their connection to ferromagnetic electrodes is fundamental to overcoming these challenges [16, 19]. A new approach introduced more than 20 years ago involves connecting molecules to two ferromagnetic metallic electrodes, with a thin insulator sandwiched between the electrodes and exposed edges. This method allows molecules to bridge via side edges, offering a wide range of electrode and insulator choices for tunnel junction-based MSD devices [20-22].

Connecting different types of molecules to various combinations of ferromagnetic electrodes can produce numerous MTJMSD alternatives. Several controlled experiments [23-25] have characterized these devices, revealing intriguing physical phenomena due to the strong exchange coupling between molecular spins and ferromagnetic electrodes. These phenomena include high current suppression at room temperature [26], spin photovoltaic effect [27], long-range magnetic ordering due to molecule [28], organic molecular channel-induced tunnel currents, and enhanced but unstable magnetoresistance [24], which is significantly different from the small magnetoresistance observed in bare MTJs [25, 26]. A high level of molecule-induced spin polarization has also been observed on MTJMSD electrodes [29], similar to the extent of spin polarization observed in nickel oxides due to atomic-scale spin filtering [30]. Additionally, the electrode configuration's dependence on MTJMSD transport behaviors has been extensively studied in the literature [25].

Previous studies predominantly utilized ferromagnetic materials as electrodes in MTJ. However, recent theoretical work has highlighted the potential of using a combination of ferromagnetic (FM) and antiferromagnetic (AFM) electrodes in MTJMSD systems [31]. In such systems, molecular spins between the electrodes demonstrate a unique alignment and coupling with the AFM electrode, offering a potential for a wide range of tunable resistance states [31]. Antiferromagnetic materials, with zero net magnetization, reduce

magnetic noise, improving the stability and precision of spintronic devices [32]. Additionally, their ultrafast spin dynamics, driven by exchange interactions between anti-aligned spins, offer a key advantage over ferromagnets [33]. Notably, earlier studies have demonstrated that SMMs grown on FeMn substrate exhibited the exchange bias due to the intrerfacial spin coupling between AFM and SMM [34, 35]. Building on these insights and guided by our theoretical findings[31],we engineered cross-junction-shaped tunnel junctions using antiferromagnetic FeMn as the bottom electrode and NiFe as the top electrode. Furthermore, by doping the MTJ with single-molecule magnets (SMM), which form robust covalent coordinative bonds with metallic electrodes, we successfully transformed the conventional MTJ into an MTJMSD [36].

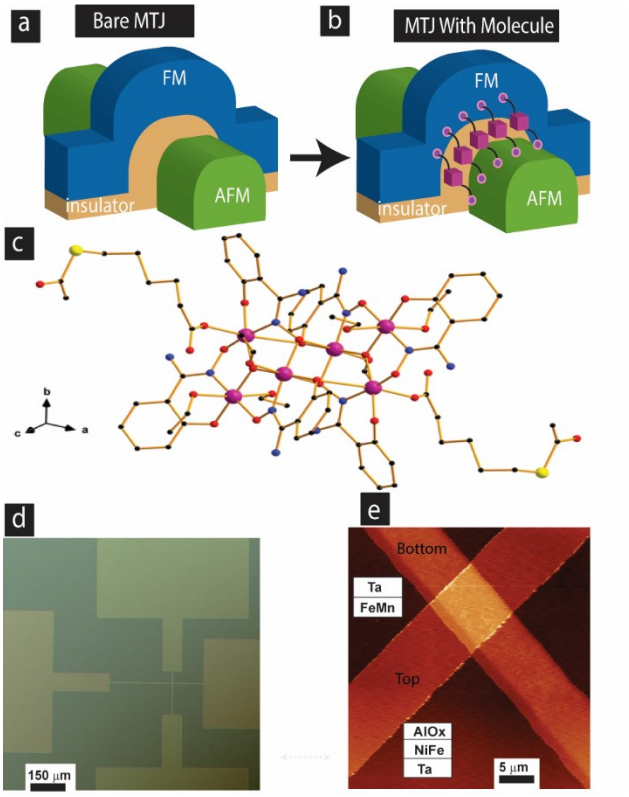

Fig.1.Schematics of the magnetic tunnel junction (a) Bare and (b) with the molecule where the bottom electrode (green) is antiferromagnet (AFM), the top (Blue) is ferromagnet (FM), and the insulator (brown) is sandwiched between them (c) Single-molecule magnet structure. (d) The photographic image of one magnetic tunnel junction (e) Atomic Force microscopy image of the same junction, where FeMn/Ta and Ta/NiFe/AlO_x represent the bottom and top electrode material stacks, respectively.

We characterized different junctions of our devices using transport measurement techniques at both room and low temperatures. Additionally, we performed low-temperature magnetization measurements on pillar-shaped devices with the same material stack and conducted Kelvin probe atomic force microscopy (KPAFM) measurements to study the work function.

Experimental Methods:

To fabricate MTJMSD devices, we utilized Single-Molecule Magnets (SMMs) as molecular channels bridging the ferromagnet-antiferromagnet electrodes of patterned MTJ cross-junction devices (Fig. 1a and b). The patterned MTJs were created using a combination of direct current (DC) and radio frequency (RF) magnetron sputter deposition techniques.

The custom-designed SMM molecule (Fig. 1c) was successfully integrated to form MTJMSD. We employed isolated cross-junction-shaped MTJs to minimize interference from neighboring devices (Fig. 1d). The MTJ was constructed with the following layer stacking structure to study the transport behavior: Ta (5 nm)/FeMn (5 nm) as the bottom electrode and AlOx (2 nm)/NiFe (5 nm)/Ta (5 nm) as the top electrode, all deposited on a thermally oxidized silicon wafer with

a 300 nm silicon dioxide layer (Fig. 1e). The AlO_x layer acts as an insulating barrier between the top and bottom electrodes, with the bottom and top Ta layers serving as the wetting and capping layers, respectively.

The Ta layers were deposited using DC sputtering, while the FeMn, AlOx, and NiFe layers were deposited using RF sputtering from stoichiometric targets. Optical and atomic force microscopy (AFM) images shown in Fig. 1d and 1e represent a single MTJMSD cross junction with an area of approximately 20 μm^2. A more comprehensive description of the experimental fabrication methods has been previously documented [37].

Results and Discussion:

Transport measurements were carried out at room temperature (300 K) on each junction of the cross-junction-shaped MTJ testbed before and after the molecule treatment, as shown in Fig. 2a and 2c. The bare junctions clearly exhibited tunneling behavior. Fig. 2a presents the transport measurements for a single junction, both bare and molecule-treated, with the latter achieving a higher current state. The highest current level observed was ~4 μA for ~50 mV, with several thousands of Single-Molecule Magnets (SMMs) bridging the two electrodes, affecting the magnetic ordering of the top and bottom electrodes. Repeated measurements for ten different MTJ junctions demonstrated consistent trends (Fig. 2c). This may be because molecules interfacing with an MTJ's magnetic electrodes influence the magnetic properties or spin density of states of magnetic electrodes [29, 38].

The increase in current in our cross-junction-based ferromagnet-antiferromagnet devices, observed in molecule-treated junctions, contrasts with the current suppression behavior in MTJMSD devices formed from both ferromagnetic electrodes in previous studies [25]. This discrepancy is likely due to the different behavior of MTJMSD systems with different electrode combinations, as theoretical studies suggest varying molecule spin orientations with different electrode types [31].

Interestingly, while all bare junctions maintained current levels around ~0.7 μA, molecule-treated junctions displayed currents ranging from ~1 μA to ~7 μA for ~60 mV input voltage (Fig. 2c). Notably, junctions 2 and 7 continued to exhibit tunneling behavior, whereas others showed significantly higher current levels post-transformation into MTJMSD. This high leakage current could potentially stem from short-circuited junctions or surface effects post-molecule treatment. To verify, I-V measurements for individual electrodes were performed (Fig. 2d), indicating that the current for antiferromagnet (H-electrode) and ferromagnet (V-electrode) electrodes remained unchanged before and after molecule treatment. This supports the idea that the observed current enhancement is intrinsic across the junction rather than due to superficial effects and short-circuited junctions.

The magnetic properties of ferromagnets and the use of SMMs as molecular channels between ferromagnet-antiferromagnet electrodes appear to enhance electron transport, likely due to SMM-induced spin filtering[39] and increased spin polarization [28, 40, 41]. This

enhancement may result from the SMM's ability to reduce scattering and facilitate coherent spin transport, as proposed in previous studies on molecular spintronics devices [42, 43]. The alignment of molecular magnetic moments with ferromagnetic electrodes might also contribute to the observed enhanced tunneling magnetoresistance (TMR) [24], warranting extensive future magneto-transport studies.

To further investigate the magnetic properties of MTJMSDs, we conducted I-V measurements in both rooms and low temperatures. Transport measurements at ~173K (Fig. 2b) were performed on a single junction before and after transformation into MTJMSD. Fig. 2b shows significant current suppression at low temperatures for the bare junction compared to the molecule-treated junction. At 40 mV, the bare junction current was recorded as 0.76 pA, while the molecule-treated junction current was ~0.23 μA. At 300 K (inset of Fig. 2a), the current levels at 40 mV were ~0.57 μA and ~3.62 μA for bare and SMM-treated samples, respectively. This data indicates that as the temperature decreases from room temperature to ~ 173 K, the bare junction's current drops from microampere to picoampere level at low temperatures, whereas the molecule-treated junction current decreases by only about tenfold.

The exact physical phenomena behind this interesting observation remain unclear. We hypothesize that the bottom electrode FeMn, with a Néel temperature close to room temperature, may exhibit pronounced antiferromagnetic ordering at lower temperatures. In FeMn alloys, the electrical conductivity tends to decrease as the temperature decreases from a high temperature due to the reduction in thermal energy. This leads to less scattering of electrons by phonons (lattice vibrations), which usually would mean higher conductivity. However, in FeMn, magnetic scattering and impurities can dominate, leading to a more complex behavior. As the temperature drops, especially in FeMn alloys with antiferromagnetic ordering, the magnetic structure significantly influences the conductivity. Antiferromagnetic materials, such as FeMn, undergo a transition at the Néel temperature, below which the electrical resistivity often increases, leading to a decrease in conductivity. This is due to the complex magnetic scattering mechanisms becoming more prominent at lower temperatures. It is noteworthy that FeMn, in our case, is only 5 nm thick and, unlike 3D bulk FeMn, more closely resembles a 2D material. Transition below Néel temperature and 3D to 2D dimensionality reduction has yielded metal-to-insulator transitions in several antiferromagnetic materials [44].

Additionally, Tantalum present under FeMn has the potential to impact the magnetic moment and other properties. In our previous study, we demonstrated the dramatic effect of Ta on the MTJMSD. We cited several cases where Ta was dominant in impacting magnetic layers deposited on top of it [45]. We surmise that FeMn has undergone a metal-to-insulating transition yielding in the pA level current at low temperatures.

We are unclear about the role of SMM in yielding ~1M higher current magnitude at 173K, while AFM electrode-based bare junction was in pA state. We surmise that SMM potentially creates efficient spin channels between the two electrodes by impacting the local magnetic

ordering on the FM and AFM electrodes, thereby significantly influencing the transport properties. In contrast to the present case, where FeMn's antiferromagnetic ordering is expected to be the cause of current suppression, SMMs were observed to transform the ferromagnetic films into semiconducting and non-magnetic materials, yielding pA-level current suppression [28]. Our hypothesis is based on our recent experimental studies showing the long-range effect of the molecules on the ferromagnetic electrodes. Magnetization studies showed that the molecule effect transformed the magnetic properties of the MTJ [46], and KPAFM studies showed that molecules also impacted the magnetic electrode work function [27]. Elsewhere in this work, we have discussed the magnetic study and KPAFM experiments with regard to the thin film stack discussed in this investigation.

Fig. 2c shows the response from 10 devices that produced the SMM effect. At 300K, SMM channels increased the tunnel junction current. However, there was a difference in the magnitude of the current increase. We surmise that we could not realize exactly the same number of SMM bridges between the two metal electrodes, leading to the difference in the magnitude of the final current. Fig. 2d shows the transport characteristics of the top and bottom electrodes before and after treating the junction with the SMMs. It is noteworthy that

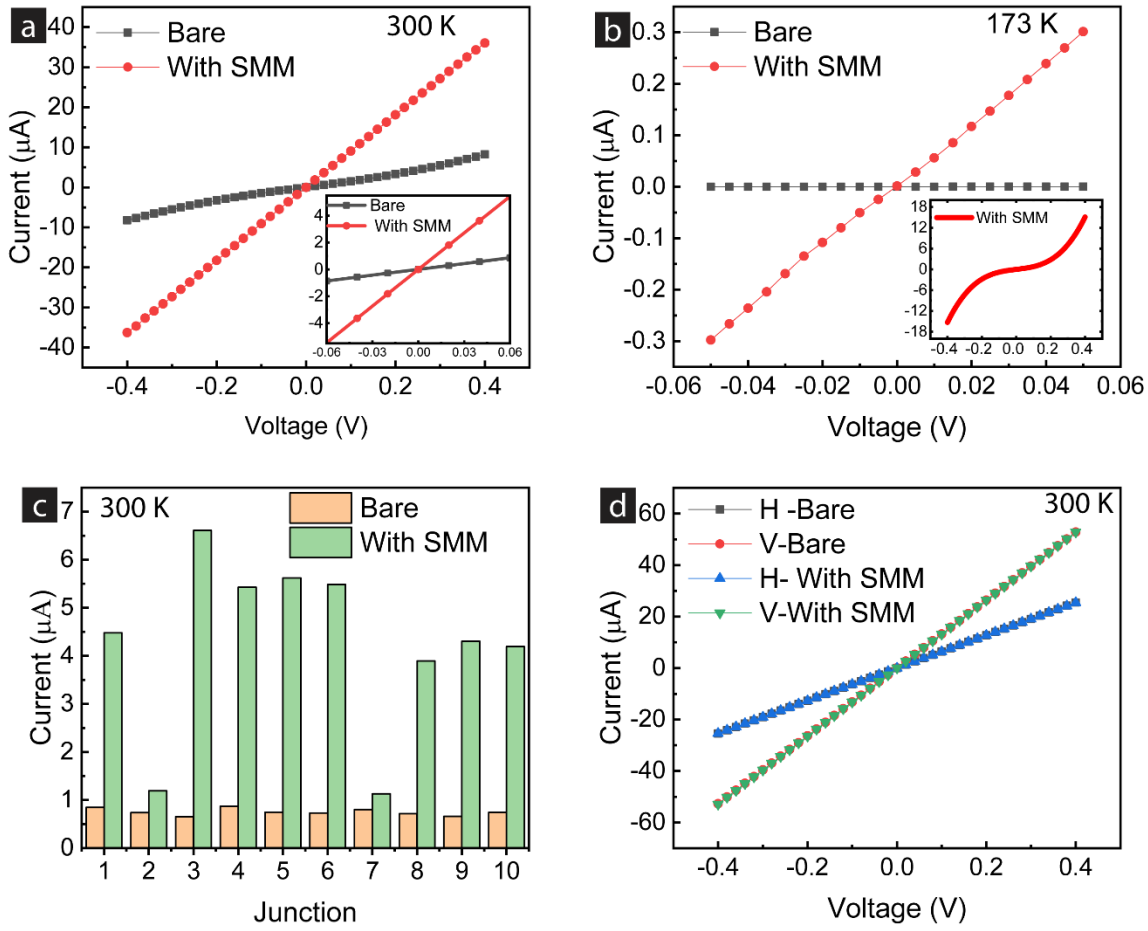

Fig. 2. Transport measurement depicting current-voltage characteristics of bare and molecule-treated samples. (a) Current as a function of applied voltage for bare (black data points) and molecule-treated samples (red data points) at 300 K. The inset of this figure represents the Zoomed in the current-voltage plot for the range -0.06 Volt to 0.06 Volt (b) Current-voltage relationship at 173 K temperature. The inset of this figure is the current Vs. voltage plot for extrapolated data from the SMM-treated sample. (c) Bar chart comparing current levels in different junctions for bare (orange bars) and molecule-treated samples (green bars) at a fixed voltage of 60 millivolts. (d) Current-voltage curves are separately shown for ferromagnetic (vertical electrodes) and antiferromagnetic (horizontal electrodes) configurations of bare and molecule-treated electrodes at 300 K. H and V denote the horizontal (antiferromagnetic) and vertical (ferromagnetic) electrodes.

only a fraction of SMM molecules form conduction bridges between the two electrodes. Metal electrodes are likely to get coated by the thiol-functionalized SMM channels (Fig.1c). Unchanged transport through two electrodes provides direct evidence that (i) SMM has not adversely impacted the metal electrodes, (ii) SMM self-assembled on the surface of the electrodes away the junction cannot form the bridges between two metal electrodes.

To gain broader and deeper insights into the SMM effect, we applied the Brinkman tunneling model as outlined in Ref. [47] to both bare and SMM-treated MTJs. To apply the Brinkman tunneling model on the experimental *J-V* data we converted the quadratic conductance vs. voltage equation in Ref. [47] into current density vs. voltage equation by integrating conductance expression with respect to voltage (Eq.1). The resultant current density $J(V)$ is expressed as a polynomial function of applied potential (V) and coefficients involving the tunneling barrier properties [47, 48]:

$$J(V) = G_0(V - \frac{A_0 e\Delta\varphi}{16\varphi^{\frac{3}{2}}}V^2 + \frac{3e^2A_0^2}{128\varphi}V^3) \quad (1)$$

where, $A_0 = \frac{8\pi(2m)^{1/2}d}{3h}$ (2)

$$G_0 = \frac{3.16\times10^{10}\exp(-1.03d\varphi^{\frac{1}{2}})}{d} \quad (3)$$

In these equations, m and e are the electron's mass and charge, respectively, h is Plank's constant, d is the barrier thickness, φ represents the average barrier height and $\Delta\varphi$ is the difference in barrier heights between two opposite sides of the junctions. Using current density-voltage (J–V) data from transport studies at two different temperatures, we fitted the 3rd order polynomial equation. The coefecients of the V, V^2, and V^3 from the fitted equation were compared with corresponding coeffecients of equation (1) to determine the barrier height and thickness for both bare and SMM-treated samples, as listed in Table 1. The bare junction exhibits a barrier thickness and height of ~1.84 nm and ~1 eV at 300 K. Bare junction barrier thickness data from the Brinkman is in excellent agreement with the expected barrier thickness of ~2 nm. Notably, the junction properties changed significantly following molecule treatment. While the bare junction demonstrated very good tunneling behavior, a purely linear response was observed after SMM treatment, as indicated by the red data points in Fig. 2a. This linearity and elevated current may arise from the alignment of the Fermi-level electrodes with the molecule, coupled with a significant reduction in barrier height and thickness following the molecular treatment. However, this linear behavior is not ideal for the Brinkman fit model, which is applicable only to the tunneling behavior of the

devices. Thus, we were unable to apply Brinkman tunneling models to quantify the barrier height and thickness for the post-molecule MTJ at 300 K.

At 173 K, the bare junction, which showed suppressed picoampere level current, exhibited the highest barrier thickness of ~4.91 nm, decreasing to ~2.25 nm after SMM treatment. Similarly, the barrier height decreased from ~0.35 eV to ~0.16 eV post-treatment. Such decrement in barrier may be the rationale for the enhancement of current at 173 K during transport measurement (Fig. 2a). Though Brinkman tunneling model is useful, but it has limitation in considering the dramatic changes in the AFM metal electrode conductivities as a function of temperature. According to prior literature, FeMn electrode material is expected to undergo a phase change to a highly ordered antiferromagnetic phase of around ~290K [49]. Since, after phase change, FeMn may exhibit a significant reduction in conductivity, we hypothesize the bare MTJ transport data at 173K is associated with FeMn phase change. Brinkman model seems to struggle in accommodating the effect of potential phase change and associated resistivity change of the FeMn and yielded a cumulative thicker barrier after modeling of Bare MTJ data at 173K. Notably, the tunneling model was originally designed for tunnel junctions without accounting for any phase change in the metal electrode. Moodera *et al*. used this tunneling model to correlate the barrier height properties to changes in magnetic electrode alignment, parallel vs anti-parallel, for investigating new materials [50]. Specifically, in our case, significant changes in barrier thickness and height are expected from the complex inter-dependence of multiple spin channels and transition in metallic electrodes. We are unable to present the full atomistic mechanism of SMM interaction with two electrodes. However, observation of tunneling transport at 173K as observed in the inset I-V data of Fig.2b on SMM-treated MTJ, suggests further change in magnetic electrodes. To verify the effect of temperature on bare MTJ and to verify the effect of SMM on bare MTJ at low temperatures, we conducted magnetic measurements.

Table 1: Barrier thickness and heights of Bare and molecule-treated samples estimated by using the Brinkman fit model.

Temperature (K)	Device Nature	Barrier Thickness (nm)	Barrier Height (eV)
300	Bare	1.84	0.99
173	Bare	4.91	0.35
173	With SMM	2.25	0.16

To confirm the role of FeMn electrode in the MTJ and MTJMSD, we conducted magnetic measurement on the group of ~10,000 cylindrical pillars. Cylindrical shape MTJ provide a direct advantage that we can avoid the effect of long magnetic electrodes extending beyond the junction area. We investigated the same material stack configuration as discussed in Fig. 1 for the cross junction, using Vibrating Sample Magnetometry (VSM). VSM measurements were performed on bare and molecule-treated MTJ devices (Fig. 3a and 3b).

The detailed experimental fabrication procedure for those devices is provided elsewhere [24]. These measurements provide insights into the magnetic properties of the SMM-treated devices. Interestingly, at room temperature (300 K), the magnetic moment of the SMM-treated samples was the same as that of the bare samples (Fig. 3a). It is noteworthy that FeMn Néel temperature is of the order of 290K [44]. Hence, it is likely that FeMn's antiferromagnetic ordering is not present for the 300K measurement. Interestingly, SMM bridging appears to produce less noisy signals, indicating some degree of cohesiveness yielded by the molecular channels. Insignificant effect on the magnetization graph also suggests SMM did not impact the metallic electrodes, which are responsible for magnetization curves.

We also studied the VSM at 55 K for bare and SMM treated MTJs. Quantum design-Versa lab free vibration sample magnetometry mode was used for our experiments. We chose 55 K to avoid any potential transition occurring at higher temperature. It is interesting to see the SMM impacted the group of ~10,000 MTJ, suggesting that we can indeed produce MTJMSD with high yield. Interestingly, the magnetic hysteresis curves, as a function of the in-plane applied field, indicate that the magnetic moment for the SMM-treated samples diminishes at a low temperature of 55 K (Fig. 3b). The mechanism behind reducing the magnetic moment of after-molecule treatment is not entirely clear to us. However, it is known that a molecule's net spin induces spin filtering [51] that prominently affects spin polarization, ultimately changing the whole system's magnetic moment. The observed VSM data resemble with our prior SQUID magnetization study on ~7000 pillars of Pd/AlO_x/NiFe cylindrical pillars before and after treating with OMC channels [31]. In the same study, we showed Monte Carlo Simulations on MTJMSD to explain the effect of molecule-induced strong exchange coupling to explain the experimental observations. We surmise that SMM produces opposite

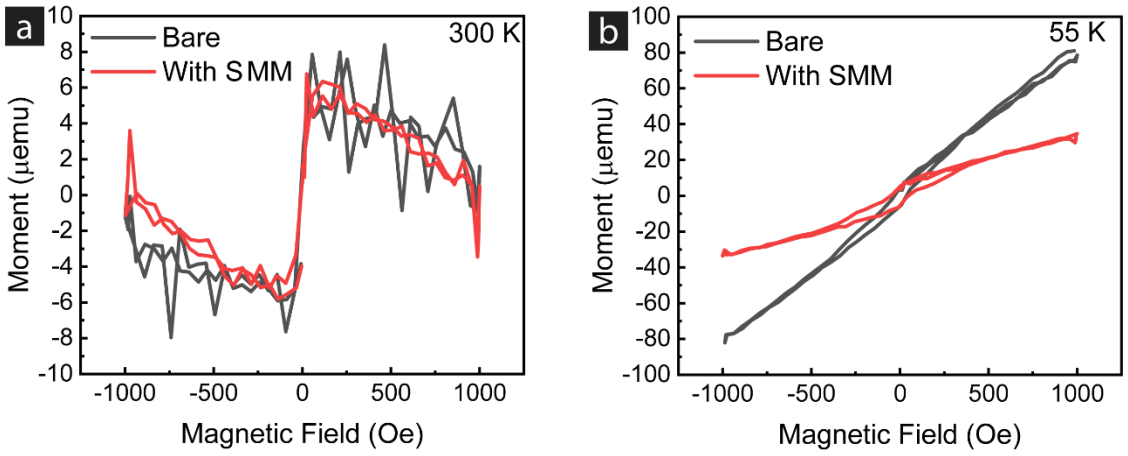

Fig. 3. Magnetic hysteresis curves for bare (black data points) and with molecule-treated (red data points) samples at (a) 300 K and (b)55 K. The magnetic moments are measured by using Quantum design-Versa lab free vibration sample magnetometer.

magnetic couplings with the two metallic electrodes and yields a spin density of state rearrangements, yielding the observed VSM response at 55K.

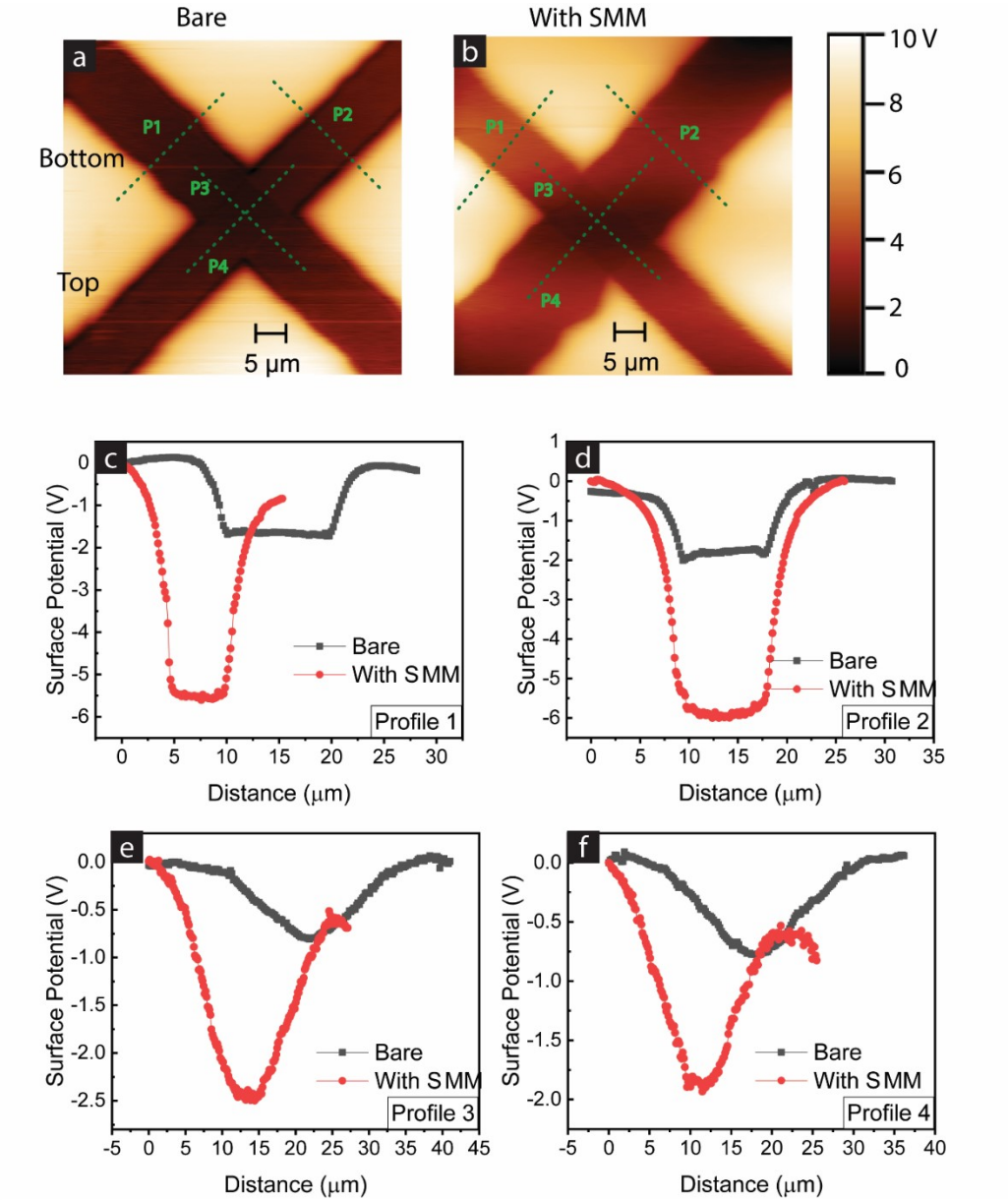

Fig.4. Kelvin Probe Atomic Force Microscopy (KPAFM) images showing (a) Bare junction and (b) Molecule treated junction. The dotted green lines P1, P2, P3 and P4 in Fig. 4a and Fig. 4b represent profiles 1, 2, 3 and 4, respectively. Profiles illustrating differential surface potential as a function of distance: (c) Surface potential of the bottom electrode before and after SMM treatment, (d) Surface potential of the top electrode before and After SMM treatment, (e) Surface potential of the junction with respect to bottom electrode before and After SMM treatment, and (f) Surface potential of the junction with respect to top electrode before and After SMM treatment. Each profile's black and red data sets in the plots represent the surface potentials for Bare and SMM-treated samples.

If molecules indeed impacted the electron density of states on the two electrodes, then we expect to observe them in the Kelvin Probe AFM(KPAFM) measurement. KPAFM can measure the surface potential and relative work function of the MTJ electrodes before and after interaction with the SMM. We conducted KPAFM on cross-junction-shaped MTJMSD to separately measure the SMM impact on top and bottom electrodes.

In previous studies, Kelvin Probe Atomic Force Microscopy (KPAFM) has been employed to investigate the effects of Single Molecule Magnets (SMMs) [52] and organometallic molecular clusters (OMCs) [27], particularly in the context of solar cell applications. Building upon this foundation, we aimed to extend these insights to our antiferromagnet-based MTJMSD system, which features a FeMn bottom layer. We conducted KPAFM measurements on both untreated and SMM-treated MTJ junctions to confirm the influence of SMM on our system (Fig. 4).

Interestingly, in ferromagnetic metal based MTJMSDs systems SMM treatment often influenced top and bottom electrodes differently [52]. It is noteworthy that in the previous studies with two FM electrodes, one FM electrode after molecule bridging impacted to the extent that it became semiconducting and started responding to light radiation. We observed minimal differences between the surface potentials of top and bottom electrodes in both untreated and treated states. This observation indicates a unique response pattern in our antiferromagnetic MTJMSD system. Further analysis involved line profiles (green dashes in Fig. 4a and 4b) across different parts of the junctions. Each profile's actual surface potential values were normalized against the highest potential within their respective datasets to ensure consistency. Profile 1 (Fig. 4c) illustrates that the bare antiferromagnetic bottom electrode was approximately 1.5 volts lower than the substrate, with a surface potential difference increasing to approximately 5.5 volts after SMM treatment. Similarly, for the top electrode (Fig. 4d), the surface potential increased from approximately 1.5 volts to around 6 volts post-treatment. Profiles 3 and 4 (Fig. 4e and 4f) illustrate the surface potential for the bottom electrode and the top electrode with reference to the junction, respectively. In the untreated state, the potential of both electrodes is very similar, approximately 0.75 volts relative to the junction. Post-SMM treatment, the bottom electrode's potential increased to approximately 2.5 volts, and the top electrode's potential increased to 1.9 volt. Additionally, Fig. 4e and 4f show an asymmetric effect of SMM on opposite sides of each junction, as shown by the red data sets. Our study on the FeMn-based MTJMSD system at room temperature demonstrates a significant effect of Single-Molecule Magnet (SMM) treatment on electrode surface potentials. Due to the limitations of AFM system, we were unable to perform KPAFM at low temperature to investigate the effect of change in magnetic ordering below Néel temperature. While earlier research primarily focused on the interaction between SMMs and ferromagnetic electrodes [52] [28] , our findings suggest that SMMs also exert a substantial influence on antiferromagnetic systems above and below Néel temperature (Fig. 2 and 3).

Conclusion:

For the first time, this study explored the impacts of Single Molecule Magnets (SMMs) on Magnetic Tunnel Junction Magnetic Spintronic Devices (MTJMSD) incorporating FeMn as an antiferromagnetic material. Cross-junction-shaped MTJMSD devices were fabricated with a structural composition comprising a bottom antiferromagnet (Ta/FeMn) and a top ferromagnet layer (AlOx/NiFe/Ta).

Transport measurements were conducted at both room temperature (300 K) and a low temperature of 173 K. Following molecule treatment, a substantial increase in current to approximately 7 microamperes was observed, signifying enhanced MTJ conductivity induced by SMMs bridging with the FeMn electrode. We also studied the effect of Néel Temperature on MTJ with and without SMM. At 173 K, the current for untreated MTJ diminished to the picoampere range, while the molecule-treated MTJ stabilized at a microampere current range. Magnetometry measurements were performed on pillar-shaped devices with the same material stack. These measurements revealed that at a lower temperature of 55 K, the magnetization decreased, although the magnetic moment remained consistent for both untreated and molecule-treated samples, albeit reduced by approximately half. Additionally, Kelvin Probe Atomic Force Microscopy (KPAFM) measurements were employed to investigate the work function. It was found that the surface potential of molecule-treated junctions increased approximately threefold compared to bare samples, demonstrating a significant long-range impact on device properties, including the FeMn electrode.

In summary, this study provides comprehensive insights into the influence of Single Molecule Magnets on FeMn-based MTJMSD structures. The observed enhancements in spin polarization, stability of electrical currents at low temperatures, and modifications in magnetic properties underscore the potential of SMMs in advancing spintronic technologies, particularly in devices incorporating antiferromagnetic materials like FeMn. Our experimental findings, combined with prior theoretical results[31], suggest that this structure may exhibit SMM induced multi-state magneto-resistance. This may arises from the spin current generated by spin-dependent electron tunneling between the ferromagnet and antiferromagnet via the SMMs. Multiple resistance states are expected to arise as SMM can transition among multiple allowable spin states—similar to the behavior observed in ferromagnet/organic-ferromagnet stacks[53]. The role of AFM electrode material can be crucial in minimizing the stray magnetic field that may adversely impact the prospect of switchability of SMM. Future work will further explore this behavior by focusing on magnetoresistance measurements of both bare and SMM-treated samples with different thin film configurations and device geometries. These findings contribute to a deeper understanding of SMM interactions in spintronics and pave the way for future applications in magnetic and electronic device development.

Author contributions: P.T. conceived the concept, while B.R.S. explored various designs and refined the existing one. J.M.L and C.R.D. provided SMM for MTJMSD research. E.P., P.S., and H.B. helped with the VSM and KPAFM experimental measurements.

Funding This research was funded by the National Science Foundation CREST Award, grant number HRD- 1914751, NSF-MRI grant 1920097, Department of Energy/ National Nuclear Security Agency (DE-FOA-0003945), NASA MUREP Institutional Research Opportunity Grant under Cooperative Agreement #80NSSC19M0196 and the Generalitat Valenciana (grant numbers AICO/2020/183 and AICO/2021/295).

Availability of data and materials Data included in this paper are available upon reasonable request.

Declarations

Conflict of interest The authors have no competing interests to declare that are relevant to the content of this article.

References:

[1] B. Chowrira *et al.*, "Quantum advantage in a molecular spintronic engine that harvests thermal fluctuation energy," *Advanced Materials,* vol. 34, no. 49, p. 2206688, 2022.

[2] M. N. Leuenberger and D. Loss, "Quantum computing in molecular magnets," *Nature,* vol. 410, no. 6830, pp. 789-793, 2001.

[3] J. Lehmann, A. Gaita-Arino, E. Coronado, and D. Loss, "Quantum computing with molecular spin systems," *Journal of materials chemistry,* vol. 19, no. 12, pp. 1672-1677, 2009.

[4] M. N. Leuenberger, F. Meier, and D. Loss, *Quantum spin dynamics in molecular magnets*. Springer, 2003.

[5] L. Bogani and W. Wernsdorfer, "Molecular spintronics using single-molecule magnets," *Nature materials,* vol. 7, no. 3, pp. 179-186, 2008.

[6] A. R. Rocha, V. M. Garcia-Suarez, S. W. Bailey, C. J. Lambert, J. Ferrer, and S. Sanvito, "Towards molecular spintronics," *Nature materials,* vol. 4, no. 4, pp. 335-339, 2005.

[7] W. Liang, M. P. Shores, M. Bockrath, J. R. Long, and H. Park, "Kondo resonance in a single-molecule transistor," *Nature,* vol. 417, no. 6890, pp. 725-729, 2002.

[8] A. Ghirri, A. Candini, and M. Affronte, "Molecular spins in the context of quantum technologies," *Magnetochemistry,* vol. 3, no. 1, p. 12, 2017.

[9] A. Cornia *et al.*, "Preparation of novel materials using SMMs," *Single-Molecule Magnets and Related Phenomena,* pp. 133-161, 2006.

[10] E. Coronado, A. Forment-Aliaga, A. Gaita-Ariño, C. Giménez-Saiz, F. M. Romero, and W. Wernsdorfer, "Polycationic Mn12 Single-Molecule Magnets as Electron Reservoirs with S> 10 Ground States," *Angewandte Chemie,* vol. 116, no. 45, pp. 6278-6282, 2004.

[11] L. Thomas, F. Lionti, R. Ballou, D. Gatteschi, R. Sessoli, and B. Barbara, "Macroscopic quantum tunnelling of magnetization in a single crystal of nanomagnets," *Nature,* vol. 383, no. 6596, pp. 145-147, 1996.

[12] W. Wernsdorfer and R. Sessoli, "Quantum phase interference and parity effects in magnetic molecular clusters," *science,* vol. 284, no. 5411, pp. 133-135, 1999.
[13] A. Ardavan *et al.*, "Will spin-relaxation times in molecular magnets permit quantum information processing?," *Physical review letters,* vol. 98, no. 5, p. 057201, 2007.
[14] N. Prokopuk and K.-A. Son, "Alligator clips to molecular dimensions," *Journal of Physics: Condensed Matter,* vol. 20, no. 37, p. 374116, 2008.
[15] R. L. Carroll and C. B. Gorman, "The genesis of molecular electronics," *Angewandte Chemie International Edition,* vol. 41, no. 23, pp. 4378-4400, 2002.
[16] P. Tyagi, "Multilayer edge molecular electronics devices: a review," *Journal of Materials Chemistry,* vol. 21, no. 13, pp. 4733-4742, 2011.
[17] A. N. Pasupathy *et al.*, "The Kondo effect in the presence of ferromagnetism," *Science,* vol. 306, no. 5693, pp. 86-89, 2004.
[18] J. R. Heath, "Molecular electronics," *Annual Review of Materials Research,* vol. 39, no. 1, pp. 1-23, 2009.
[19] E. Coronado, M. Clemente-León, J. R. Galán-Mascarós, C. Giménez-Saiz, C. J. Gómez-García, and E. Martínez-Ferrero, "Design of molecular materials combining magnetic, electrical and optical properties," *Journal of the Chemical Society, Dalton Transactions,* no. 21, pp. 3955-3961, 2000.
[20] G.-X. Miao, M. Münzenberg, and J. S. Moodera, "Tunneling path toward spintronics," *Reports on Progress in Physics,* vol. 74, no. 3, p. 036501, 2011.
[21] J. S. Moodera, J. Nassar, and G. Mathon, "Spin-tunneling in ferromagnetic junctions," *Annual Review of Materials Science,* vol. 29, no. 1, pp. 381-432, 1999.
[22] S. Parkin, "Spin-polarized current in spin valves and magnetic tunnel junctions," *MRS bulletin,* vol. 31, no. 5, pp. 389-394, 2006.
[23] P. Tyagi, D. Li, S. M. Holmes, and B. J. Hinds, "Molecular electrodes at the exposed edge of metal/insulator/metal trilayer structures," *Journal Of The American Chemical Society,* vol. 129, no. 16, pp. 4929-4938, 2007.
[24] P. Tyagi and E. Friebe, "Large resistance change on magnetic tunnel junction based molecular spintronics devices," *Journal of Magnetism and Magnetic Materials,* vol. 453, pp. 186-192, 2018.
[25] M. Savadkoohi, C. D'Angelo, A. Grizzle, B. Dahal, and P. Tyagi, "Impact of ferromagnetic electrode length and thickness on Magnetic Tunnel Junction-Based Molecular Spintronic Devices (MTJMSD)," *Organic Electronics,* vol. 102, p. 106429, 2022/03/01/ 2022, doi: https://doi.org/10.1016/j.orgel.2022.106429.
[26] P. Tyagi, C. Riso, and E. Friebe, "Magnetic Tunnel Junction Based Molecular Spintronics Devices Exhibiting Current Suppression At Room Temperature," *Organic Electronics,* vol. 64, pp. 188-194, 2019.
[27] P. Tyagi and C. Riso, "Molecular spintronics devices exhibiting properties of a solar cell," *Nanotechnology,* vol. 30, no. 49, p. 495401, 2019.
[28] P. Tyagi and C. Riso, "Magnetic force microscopy revealing long range molecule impact on magnetic tunnel junction based molecular spintronics devices," *Organic Electronics,* vol. 75, p. 105421, 2019.

[29] P. K. Tyagi, C. Baker, and C. D'Angelo, "Paramagnetic molecule induced strong antiferromagnetic exchange coupling on a magnetic tunnel junction based molecular spintronics device," *Nanotechnology,* vol. 26, 2015.
[30] R. Vardimon, M. Klionsky, and O. Tal, "Indication of complete spin filtering in atomic-scale nickel oxide," *Nano letters,* vol. 15, no. 6, pp. 3894-3898, 2015.
[31] E. Mutunga, C. D'Angelo, and P. Tyagi, "Magnetic molecules lose identity when connected to different combinations of magnetic metal electrodes in MTJ-based molecular spintronics devices (MTJMSD)," *Scientific Reports,* vol. 13, no. 1, p. 16201, 2023/09/27 2023, doi: 10.1038/s41598-023-42731-9.
[32] D. Xiong *et al.*, "Antiferromagnetic spintronics: An overview and outlook," *Fundamental Research,* vol. 2, no. 4, pp. 522-534, 2022.
[33] V. Baltz, A. Manchon, M. Tsoi, T. Moriyama, T. Ono, and Y. Tserkovnyak, "Antiferromagnetic spintronics," *Reviews of Modern Physics,* vol. 90, no. 1, p. 015005, 2018.
[34] A. Lodi Rizzini *et al.*, "Exchange biasing single molecule magnets: coupling of TbPc2 to antiferromagnetic layers," *Nano letters,* vol. 12, no. 11, pp. 5703-5707, 2012.
[35] C. Nistor *et al.*, "Exchange bias of TbPc 2 molecular magnets on antiferromagnetic FeMn and ferromagnetic Fe films," *Physical Review B,* vol. 92, no. 18, p. 184402, 2015.
[36] C. Rojas-Dotti and J. Martínez-Lillo, "Thioester-functionalised and oxime-based hexametallic manganese (III) single-molecule magnets," *RSC advances,* vol. 7, no. 77, pp. 48841-48847, 2017.
[37] P. Tyagi, "Fabrication of tunnel junction-based molecular electronics and spintronics devices," *Journal of Nanoparticle Research,* vol. 14, pp. 1-15, 2012.
[38] M. Galbiati, *Molecular spintronics: from organic semiconductors to self-assembled monolayers*. Springer, 2015.
[39] X. Hao, J. Moodera, and R. Meservey, "Spin-filter effect of ferromagnetic europium sulfide tunnel barriers," *Physical review B,* vol. 42, no. 13, p. 8235, 1990.
[40] C. Tiusan *et al.*, "Spin filtering effects in monocristalline Fe/MgO/Fe magnetic tunnel junctions," *Materials Science and Engineering: B,* vol. 126, no. 2-3, pp. 112-119, 2006.
[41] S. Joo *et al.*, "Spin-filtering effect of thin Al2O3 barrier on tunneling magnetoresistance," *Applied Physics Letters,* vol. 104, no. 15, 2014.
[42] L. Guo, Y. Qin, X. Gu, X. Zhu, Q. Zhou, and X. Sun, "Spin transport in organic molecules," *Frontiers in Chemistry,* vol. 7, p. 428, 2019.
[43] D. Li and G. Yu, "Innovation of materials, devices, and functionalized interfaces in organic spintronics," *Advanced Functional Materials,* vol. 31, no. 28, p. 2100550, 2021.
[44] *Solid State Inorganic Chemistry* (Comprehensive Inorganic Chemistry III (Third Edition)). Elsevier, 2023.
[45] P. Tyagi and T. Goulet, "Nanoscale Tantalum layer impacting magnetic properties of tunnel junction-based molecular devices," *MRS Comm.,* vol. 8, no. 3, pp. 1024-1028, 2018, doi: 10.1557/mrc.2018.132.

[46] P. Tyagi, C. Baker, and C. D'Angelo, "Paramagnetic Molecule Induced Strong Antiferromagnetic Exchange Coupling on a Magnetic Tunnel Junction Based Molecular Spintronics Device," *Nanotechnology,* vol. 26, p. 305602, 2015.
[47] W. Brinkman, R. Dynes, and J. Rowell, "Tunneling conductance of asymmetrical barriers," *Journal of applied physics,* vol. 41, no. 5, pp. 1915-1921, 1970.
[48] W. Guo, "Compact Modeling of Magnetic Tunnel Junctions and Design of Hybrid CMOS-magnetic Integrated Circuits," 2010.
[49] P. La Roca, P. Marinelli, A. Baruj, M. Sade, and A. F. Guillermet, "Composition dependence of the Néel temperature and the entropy of the magnetic transition in the fcc phase of Fe-Mn and Fe-Mn-Co alloys," *Journal of Alloys and Compounds,* vol. 688, pp. 594-598, 2016.
[50] M. Müller, G.-X. Miao, and J. S. Moodera, "Thickness dependence of ferromagnetic- and metal-insulator transition in thin EuO films," *Journal of applied physics,* vol. 105, no. 7, 2009.
[51] P. N. Abufager, R. Robles, and N. Lorente, "FeCoCp3 molecular magnets as spin filters," *The Journal of Physical Chemistry C,* vol. 119, no. 22, pp. 12119-12129, 2015.
[52] M. Savadkoohi, D. Gopman, P. Suh, C. Rojas-Dotti, J. Martínez-Lillo, and P. Tyagi, "Spin solar cell phenomenon on a single-molecule magnet (SMM) impacted CoFeB-based magnetic tunnel junctions," *ACS Applied Electronic Materials,* vol. 5, no. 6, pp. 3333-3339, 2023.
[53] G. Hu, M. Zuo, Y. Li, J. Ren, and S. Xie, "Multi-state magnetoresistance in ferromagnet/organic-ferromagnet/ferromagnet junctions," *Applied Physics Letters,* vol. 104, no. 3, 2014.